ENTOMOLOGICAL SOCIETY OF AMERICA
SHARING INSECT SCIENCE GLOBALLY

OXFORD

Comparative Lipid Profile Analysis of *Hermetia illucens* Larvae Fed Food Waste at Different Days of Age Using an LC-MS-Based Lipidomics Approach

Mengmeng Li, Guiying Wang, Rongsheng Shang, Qinglong Xu, Jincheng Zhang, Ran Sun, and Lusheng Li[1],

College of Agronomy, Liaocheng Research Institute of Donkey High-Efficiency Breeding and Ecological Feeding, Liaocheng University, Liaocheng 252000, China and [1]Corresponding author, e-mail: lushengli1974@126.com

Abstract

A lipidomics approach based on liquid chromatography–tandem mass spectrometry (LC-MS) was applied to analyze the molecular-level mechanism of lipid deposition in *Hermetia illucens* (*H. illucens*) larvae fed food waste (FW) at different days of age. The *H. illucens* larvae reared on FW substrates generally became larger, heavier, and fatter at 5–15 d of age. A large amount of glycerolipids (GL) were deposited, while glycerophospholipids (GP), sphingolipids, and derivatized lipids became relatively less abundant during the growth stage of the larvae. Forty-three subclasses of 3,205 lipid molecules were identified in larvae, and 139 lipids (79 upregulated and 60 downregulated during larval growth and development) were identified as potential biomarkers (variable importance in projection > 1; $P < 0.05$). The differential lipids were mainly enriched in 19 metabolic pathways, of which 9 metabolic pathways related to lipids, including GL and GP metabolisms. The results demonstrate that the lipid composition and mechanisms changed during the growth and development stage of *H. illucens* larvae. To the best of our knowledge, this is the first work exploring the molecular-level mechanism of lipid deposition during the growth and development stage of *H. illucens* larvae. The findings provide novel information for determining and utilizing the nutritional value of *H. illucens* larvae.

Graphical Abstract
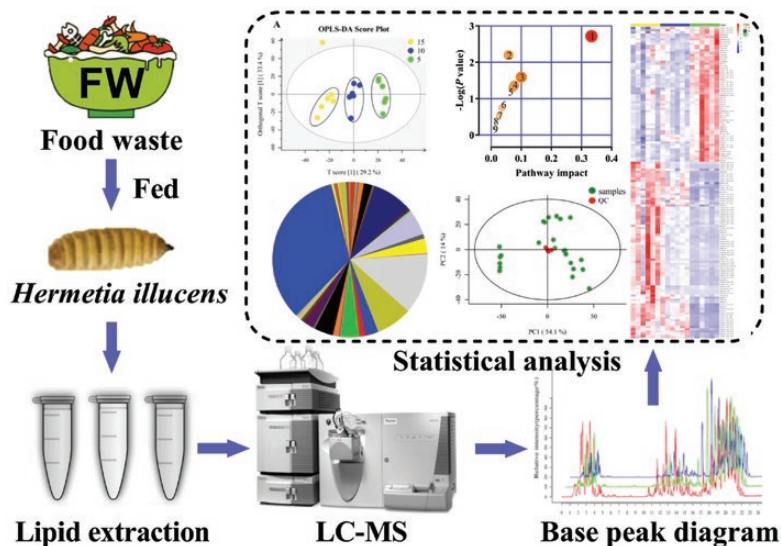
LC-MS-based lipidomics is a powerful tool for the lipid profile analysis of *Hermetia illucens* larvae.

Key words: *Hermetia illucens*, food waste, lipid profile, lipidomics, growth stage

With the rapid development of society and medicine, the world population is expected to reach nine billion by 2050 (Gerber et al. 2013). As a result, there is a growing demand for meat, eggs, and milk (Philippe et al. 2015). Currently, approximately 1.3 billion tons of food waste (FW) is generated each year, accounting for one-third of the food produced for human consumption. Given the growing demand for feed and food, the development of new renewable resources has become a critical issue worldwide. Insects can eat waste and are rich in protein and oil (Dobermann et al. 2017), making them a promising new feed source with the potential to reduce environmental pressures.

In recent years, the bright spotted flat horned *Hermetia illucens*, L. (*H. illucens*, 1758, Hermetia (Diptera: Stratiomyiidae), Insecta) has attracted particular attention dues to its fast growth, short reproduction cycle, high rate of conversion of protein and lipid, large biomass, and diverse food sources/substrates, and its potential role in waste management (Wang et al. 2017, Surendra et al. 2020). Previous studies have suggested that wastes such as fresh pig manure, goat manure, quail manure, chicken manure (El-Dakar et al. 2021), FW (Chu et al. 2020, Guo et al. 2020), and industrial *Schizochytrium microalgal sp.* (S31, Thraustochytriaceae) waste (El-Dakar et al. 2020), can be used as substrates for *H. illucens* larvae. The nutritional value of *H. illucens* larvae depends on its food source (Surendra et al. 2020, El-Dakar et al. 2021). *H. illucens* larvae meal has been successfully used as feed for pets and livestock such as poultry, swine, and fish (Belghit et al. 2019, Bosch et al. 2014, Yu et al. 2019, Chu et al. 2020). Therefore, *H. illucens* biotreatment is regarded as an environmentally friendly alternative for organic waste disposal as *H. illucens* can efficiently convert waste into feedstocks.

Food waste is produced throughout the food supply chain (production, processing, distribution, storage, sale, preparation, cooking, and serving), primarily via the loss or waste of food during processing and consumption (Gustavsson et al. 2011). However, FW is sometimes used specifically for the consumer stage, such as homes, restaurants, and school and hospital cafeterias (Parfitt et al. 2010). Compared to other organic wastes (e.g., livestock manure), fats and oils account for a larger proportion of FW, and the pollution caused by FW is more serious (Gustavsson et al. 2011, He et al. 2012). The methods for treating FW include landfilling, incineration, anaerobic digestion, feed conversion, and bioconversion (Xu et al. 2018, Guo et al. 2020). Bioconversion refers to the use of organisms to convert FW into biological proteins, oils, and organic fertilizers. Thus, bioconversion is a convenient and simple method for processing FW with low secondary pollution and high economic value added (Uçkun Kiran et al. 2014, Salomone et al. 2017). *H. illucens* larvae can fully digest and utilize the fats in FW and convert them into their own fat for storage in the body (Wang et al. 2019). The fat levels and fatty acid profiles of *H. illucens* biomass have been reported for *H. illucens* reared on different organic wastes (Rabani et al. 2019, Surendra et al. 2020). However, the development of the lipid profile as *H. illucens* transform themselves with FW remains poorly understood.

Since lipidomics was proposed in 2003 (Han et al. 2003), it has been frequently used in studies on metabolic diseases, nutritional health, and food science (Han 2016, Sun et al. 2020). Lipidomics makes it possible to accurately describe species, structures, and fatty acid chain lengths of lipid molecules in cells and tissues at the molecular level, thereby revealing the compositions and functions of lipids in biological metabolic processes (Griffiths et al. 2009). However, lipidomics has rarely been applied to the study of *H. illucens* lipids. In addition, although several studies have reported the fat content and fatty acid profiles of *H. illucens* larvae (Ewald et al. 2020, El-Dakar et al. 2021), a more comprehensive lipidomic profile analysis of larvae, specifically lipid profile of larvae fed food waste at different days of age, has not been carried out. Therefore, the objective of the present study was to assess growth performance, as well as content, classes, differential molecular and metabolism pathways of lipids in *H. illucens* larvae reared on FW substrates at different days of age using a lipidomics approach based on liquid chromatography–tandem mass spectrometry (LC-MS).

Materials and Methods

Food Waste and Experimental Design

Food waste was obtained from the cafeteria of Liaocheng University. After the solid and liquid components of the FW were separated, the solid was ground into a uniform slurry with a homogenizer and stored at –20°C for later use. The crude fat content of the FW was determined to be 10.2% ± 0.52% (dry matter basis). The predominant lipid classes in FW were determined to be triglycerides (TG; 66.76%), phosphatidylcholines (PC; 13.19%), sphingomyelin (SM; 3.90%), methyl phosphatidylcholine (MePC; 2.91%), phosphatidylethanolamine (PE; 2.35 %), and diglyceride (DG; 2.32%; Table 1).

One-day-old BSF larvae (180 g) were purchased from Shandong Wooneng Agricultural Science and Technology Co., Ltd. (Liaocheng, China) and randomly divided into six containers (1.0 × 1.0 × 0.25 m) according to weight, 30 g per container. The remaining amount of FW was observed and then added enough FW to ensure that larvae were able to feed ad libitum every day, and the feeding trial lasted for 15 d. The temperature was maintained at 28°C ± 2°C, and the relative humidity was 60% ± 3%.

Sample Collection

The larvae were collected on days 5, 10, and 15 after the start of the experiment (corresponding to 5-, 10-, and 15-d-old larvae, respectively), and 30 individual larvae were weighed using a microscale analytical balance (Sartorius, Beijing, China). Their body lengths and diameters were measured using Vernier calipers (Haogonggong Measuring Tools Co., Ltd., Shanghai, China). Larvae (approximately 10.0 g) were randomly collected from each container, sealed in vacuum-packed bags, and stored at –20°C for measurement of crude fat. Approximately 2.0 g of larvae from each container were randomly collected, added to 2.0 ml centrifuge tubes, and stored at –80°C for measurement of the lipid profile.

Analysis of Crude Fat

Crude fat was analyzed using the Soxhlet petroleum ether extraction method as previously reported (El-Dakar et al. 2020). Briefly, 1 g of larvae meal was subjected to Soxhlet extraction at 65°C for 4 h using petroleum ether as the solvent. The flask containing fat was dried for 1 h at 105°C and cooled in a desiccator at room temperature for 30 min before weighing the fat. The crude fat content was expressed as a weight percentage of dry matter.

Lipid Extraction

Each 100 mg sample was placed into 2-ml centrifuge tubes followed by the addition of 750 µl chloroform:methanol (2:1; precooled at –20°C) and two steel balls (Li et al. 2021b). The samples were ground using a high-flux tissue grinder (SCIENTZ-48, Xinzhi Biological Technology Co., Ltd. Ningbo, China) for 120 s at 60 Hz. Subsequently, 190 µl ddH$_2$O was added to the mixture, which was

Table 1. Relative lipid contents in the experimental diet and *Hermetia illucens* larvae at different days of age based on lipidomics analysis (%)

Lipid	Diet	Larvae at different days of age			SEM	*P* value
	FW	5	10	15		
TG	66.7624	67.5033[a]	74.9616[b]	75.4005[b]	1.1054	0.001
PC	13.1921	11.1548[b]	7.1629[a]	6.4298[a]	0.5786	0.000
PE	2.3520	2.8829[b]	1.8855[a]	1.6943[a]	0.1522	0.000
DG	2.3180	1.5800[a]	2.2081[b]	3.5300[c]	0.2112	0.000
SM	3.9013	4.4580	5.0207	4.3312	0.1678	0.221
Cer	1.5480	2.8463[b]	1.8779[a]	1.6803[a]	0.1398	0.000
MePC	2.9071	1.4246[b]	1.1501[a]	0.9945[a]	0.0633	0.009
BisMePA	1.2638	1.7520[b]	1.0691[a]	0.8665[a]	0.1090	0.000
PA	0.0256	0.0107[a]	0.0100[a]	0.0217[b]	0.0018	0.006
PG	1.0570	0.3384	0.3098	0.2999	0.0092	0.217
PI	0.6181	0.1646	0.1250	0.1354	0.0087	0.161
PS	0.1156	0.1652[b]	0.1007[a]	0.1196[a]	0.0104	0.023
AcCa	0.0636	1.7662[c]	1.3332[b]	0.9364[a]	0.1038	0.001
Co	0.1473	0.4813[b]	0.4574[b]	0.2535[a]	0.0308	0.001

TG: triglyceride, PC: phosphatidylcholine, PE: phosphatidylethanolamine, DG: diacylglycerol, SM: sphingomyelin, Cer: ceramide, MePC: methyl phosphatidylcholine, BisMePA: bis-methyl phosphatidic acid, PA: phosphatidic acid, PG: phosphatidylglycerol, PI: phosphatidylinositol, PS: phosphatidylserine, AcCa: acyl carnitine, Co: coenzyme.

Values are means and standard error of the mean (SEM) ($n = 6$). Values with different letters are significantly different ($P < 0.05$).

then stored on ice for at least 1 h. The sample was then vortex-mixed and centrifuged at 12,000 ×g for 5 min at 4°C. The resultant supernatant was concentrated to dryness under vacuum. The sample was dissolved with 200 μl isopropanol, filtered through a 0.22 μm polyvinylidene fluoride membrane, and stored at –20°C for LC-MS analysis.

LC-MS Analysis

Chromatographic separation was accomplished using a liquid chromatography system (Ultimate 3000 system, Thermo Fisher Scientific, MA) equipped with an Acquity UPLC BEH C18 column (100 × 2.1 mm, 1.7 μm; Waters, Thermo Fisher Scientific) column maintained at 50°C. The temperature of the autosampler was 8°C. Gradient elution was carried out with acetonitrile/water (60/40, v/v) with 0.1% formic acid and 10 mM ammonium formate (C) and isopropanol/acetonitrile (90/10, v/v) with 0.1% formic acid and 10 mM ammonium formate (D) at a flow rate of 0.25 ml/min. Each 2-μl sample was injected after equilibration. The gradient elution program was as follows: 0–5 min, 70–57% C; 5–5.1 min, 57–50% C; 5.1–14 min, 50–30% C; 14–14.1 min, 30% C; 14.1–21 min, 30–1% C; 21–24 min, 1% C; 24–24.1 min, 1–70% C; and 24.1–28 min, 70% C.

Mass spectrometry (MS) was carried out using a Thermo Q Exactive Focus (Thermo Fisher Scientific) spectrometer with spray voltages of 3.5 and –2.5 kV in the positive and negative modes, respectively. The sheath gas and auxiliary gas were set at 30 and 10 arbitrary units, respectively. The capillary temperature was 325°C. For the full scan, the mass-to-charge ratio (*m/z*) range of 150–2,000 was scanned using an Orbitrap analyzer at a mass resolution of 35,000. Data-dependent acquisition MS/MS experiments were performed with HCD scan. The normalized collision energy was 30 eV. Dynamic exclusion was implemented to remove unnecessary information from the MS/MS spectra.

Statistical Analysis

The raw data obtained using LipidSearch software (v4, Thermo Fisher Scientific) were annotated based on the Lipid Structure Database (LMSD; http://www.lipidmaps.org/. The resulting dataset included *m/z*, retention time (RT), and peak response value (intensity). Information data matrix. Alignment was performed using LipidSearch software (v4.0, Thermo Fisher Scientific). Peak alignment and peak filtering were performed on the annotation results of all single data points with an RT tolerance of 0.25 and an m-score threshold of 3. Data were analyzed by one-way analysis of variance (ANOVA) and Tukey's test using SAS software (v9.2, SAS Institute Inc., Cary, NC). Values of *P* less than 0.05 were considered to indicate significant differences. Data were assessed using principal component analysis (PCA) and orthogonal partial least squares discriminant analysis (OPLS-DA) were performed to discriminate the samples. The lipid molecules with variable importance in projection (VIP) values greater than 1 and *P* values less than 0.05 were identified as statistically significant.

Results

Growth Performance and Crude Fat

As was shown in Fig. 1, the body weights (Fig. 1A) and diameters (Fig. 1C) of larvae increased linearly with increasing days of age ($P < 0.01$). Larvae body length was significantly higher ($P < 0.01$) at days 10 and 15 than at day 5 (Fig. 1B), whereas there was no significant difference in length between 10- and 15-d-old larvae ($P > 0.05$). The levels of crude fat were significantly increased from days 5 to 15 (Fig. 1D).

Lipid Profiles

The qualitative lipid analyses achieved excellent separation in FW and *H. illucens* larvae (Supp Figs. S1A and B [online only]). The quality control samples were plotted in a concentrated area in the PCA score plots (Supp Fig. S2 [online only]). The numbers of samples and lipid classes are shown in Supp Table S1 (online only) and Fig. 2. In both FW and larvae, 43 subclasses of 3,205 lipids (Supp Table S1 [online only]) were identified by searching the *m/z* against the LMSD. These lipid molecules can be divided into three main lipid categories: glycerolipids (GLs), glycerophospholipids
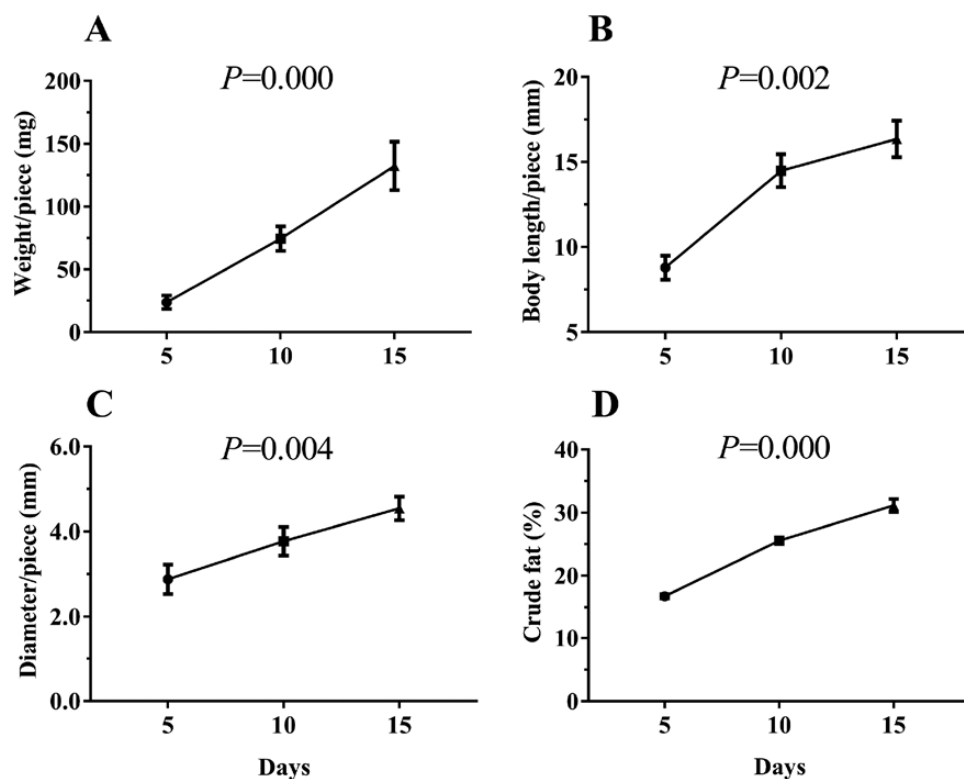
Fig. 1. Blots of body weight (A), length (B), diameter (C), and crude fat content (D) in *Hermetia illucens* larvae at different days of age (*n* = 30).

(GPs), and sphingolipids (SPs). There were three subclasses of GLs: TG (33.85%), DG (5.21%), and monoglyceride (MG; 0.22%). There were seven subclasses of GPs: PC (12.70%), PE (7.55%), PG (2.78%), cardiolipin (CL; 1.81%), PS (1.22%), PI (1.75%), and PA (0.44%). There were four subclasses of SPs: ceramide (Cer; 8.49%), SM (4.02%), hexosylceramide (HexCer; 3.09%), ceramides GGNA (CerGGNAc; 0.19%), and sphingosine (SPH; 0.47%; Fig. 2).

As was shown in Table 1, the predominant lipid class in *H. illucens* larvae was TG (67.50–75.40%) followed by PC (6.43–11.15%) and SM (4.33–5.02%). The relative proportions of TG and DG in 10- and 15-d-old larvae were significantly higher than those in 5-d-old larvae (*P* < 0.01), whereas the opposite trends were found for PC, PE, Cer, MePC, bis-methyl phosphatidic acid (BisMePA), PS, and acyl carnitine (AcCa). The relative SM contents showed no significant difference in all groups (*P* > 0.05).

Differential Lipid Molecules

As was shown in Fig. 3, the OPLS-DA score plots for larvae at different ages are clearly separated, and the verification parameters were $R^2X = 0.716$, $R^2Y = 0.970$, and $Q^2 = 0.881$ in ion mode (Fig. 3A). The corresponding OPLS-DA validation plots [R^2 = (0.0, 0.67), Q^2 = (0.0, –0.46)] in (Fig. 3B).

As was shown in Supp Table S2 (online only), a total of 139 significantly different lipids were identified: three AcCas, three BisMePAs, one CL, three CarEs, four Cers, four DGs, two hexosylceramides (Hex1Cers), four lysophosphatidylcholines (LPCs), one lysosphingomyelin (LSM), three MePCs, 12 PCs, five PEs, one PG, seven SMs, one stigmasterol ester (StE), 80 TGs, three zymosterol esters (ZyEs), and two sulfoquinovosyldiacylglycerols (SQDGs) (VIP > 1; *P* < 0.05). The 139 lipids were differentially regulated in the 15-d-old vs. 10-d-old vs. 5-d-old groups: 79 upregulated

(62 TGs, four DGs, one StE, three ZyEs, four SMs, two MePCs, one PC, one LPC, and one AcCa) and 60 downregulated (two AcCas, three BisMePAs, one CL, three CarEs, four Cers, two Hex1Cers, three LPCs, one LSM, one MePCs, 11 PCs, five PEs, one PG, four SMs, 18 TGs, and two SQDGs) (Fig. 4).

Metabolism Pathways

Enrichment analysis was carried out on 139 different lipids of larvae at different ages using the Kyoto encyclopedia of genes and genomes (KEGG) database. As was shown in Fig. 5A, a total of 19 major metabolic pathways were enriched, including arachidonic acid, GP, alpha-linolenic acid, GL, and linoleic acid metabolism, and vitamin digestion and absorption. According to pathway impact, 9 metabolic pathways related to lipids, including glycosylphosphatidylinositol (GPI)-anchor biosynthesis, GP metabolism, cholesterol metabolism, fat digestion and absorption, regulation of lipolysis in adipocytes, linoleic acid metabolism, GL metabolism, alpha-linolenic acid metabolism, and arachidonic acid metabolism (Fig. 5B).

Discussion

In the present study, the growth performance and crude fat content of FW-fed *H. illucens* larvae at different ages were assessed. The body weights and diameters of larvae increased linearly with increasing days of age. This result was consistent with the reported that *H. illucens* larvae generally became larger and heavier over the course of development (El-Dakar et al. 2021). Larvae body length was significantly higher at days 10 and 15 than at day 5, whereas there was no significant difference in length between 10- and 15-d-old larvae. These results indicate that the length of larvae did not increase significantly from days 10 to 15, inconsistent with a previous
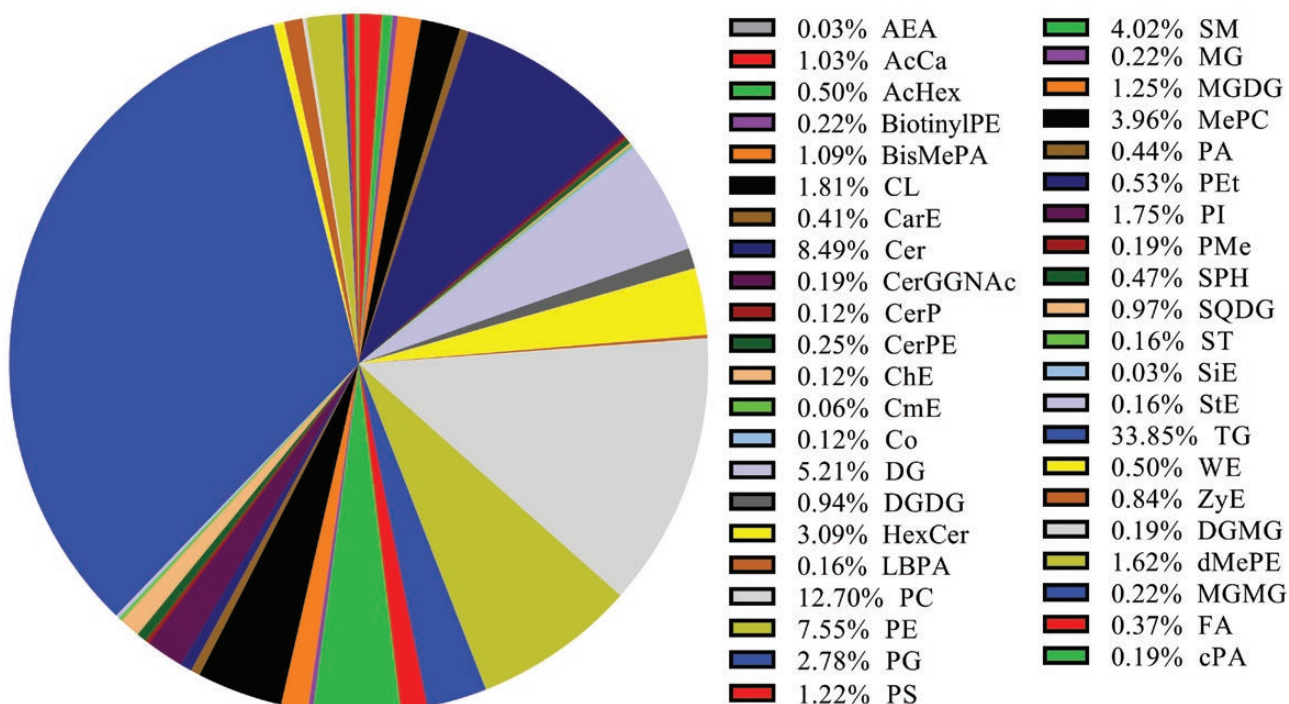
Fig. 2. Lipid profile of *Hermetia illucens* larvae. AEA: N-acylethanolamine, AcCa: acyl carnitine, AcHex: aerosol characterization experiment, BiotinylPE: glycerophosphoethanolamine-N-(biotinyl), BisMePA: bis-methyl phosphatidic acid, CL: cardiolipin, Cer: ceramides, CerGGNAc: ceramides GGNAc, CerP: ceramides phosphate, CerPE: ceramide phosphoethanolamines, ChE: cholesterol ester, CmE: campesterol ester, Co: coenzyme, DG: diglyceride, DGDG: digalactosyldiacylglycerol, HexCer: hex ceramides, LBPA: LB phosphatidic acid, PC: phosphatidylcholine, PE: phosphatidylethanolamine, PG: phosphatidylglycerol, PS: phosphatidylserine, SM: sphingomyelin, MG: monoglyceride, MGDG: monogalactosyldiacylglycerol, MePC: methyl phosphatidylcholine, PA: phosphatidic acid, PEt: phosphatidylethanol, PI: phosphatidylinositol, PMe: phosphatidylmethanol, SPH: sphingosine, SQDG: sulfoquinovosyldiacylglycerol, ST: sulfatide, SiE: sitosterol ester, TG: triglyceride, WE: wax ester, ZyE: zymosterol ester, DGMG: digalactosylmonoacylglycerol, dMePE: dimethylphosphatidylethanolamine, MGMG: monogalactosylmonoacylglycerol, FA: fatty acid, cPA: cyclic phosphatidic acid.
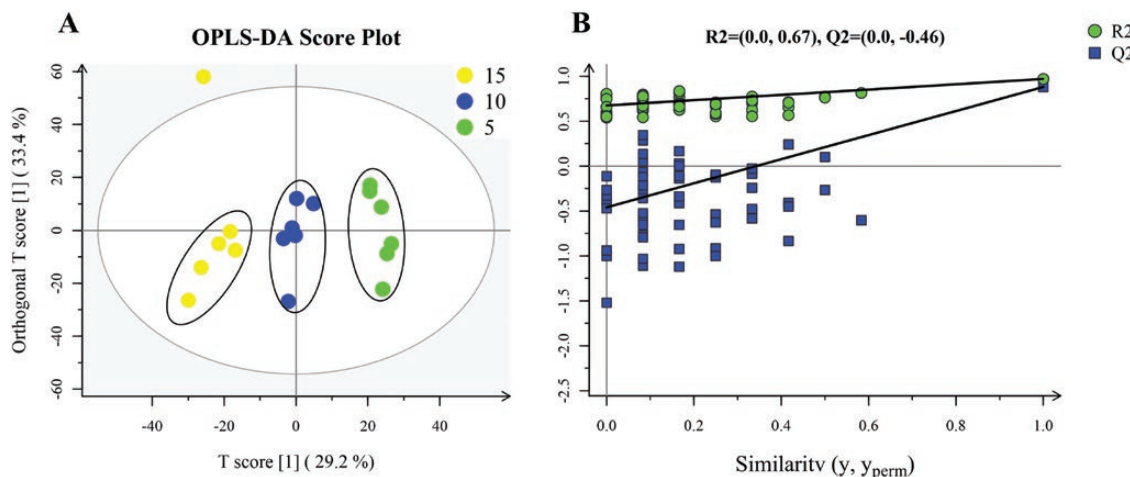

Fig. 3. (A) OPLS-DA score plot based on the lipidomic data in *Hermetia illucens* larvae in the 5-, 10-, and 15-d-old groups ($R^2X = 0.716$, $R^2Y = 0.970$, $Q^2 = 0.881$) and (B) the corresponding OPLS-DA validation plots [$R^2 = (0.0, 0.67)$, $Q^2 = (0.0, -0.46)$].

report (El-Dakar et al. 2021). Instead, the larvae may have mainly gained fat to increase their weight during this period. This is confirmed by the increase in the levels of crude fat from days 5 to 15 in this study. The insect growth rate is thought to be governed primarily by the nutrient profile and diet composition (Haas et al. 2006, Trinh et al. 2013), which supports the present results. Compared to livestock and poultry manure, FW is rich in nutrients; thus, the larvae

grew rapidly in the early stage of development and grew more slowly while accumulating more fat in the later stage (Lalander et al. 2019).

In the present study, 43 subclasses of 3,205 lipids were identified in FW and *H. illucens* larvae. These results were significantly higher than those found in pork and chicken (About 1,200 lipid species) in previous studies (Mi et al. 2018, Mi et al. 2019). These results confirm that *H. illucens* larvae are rich in lipid species. The reasonable
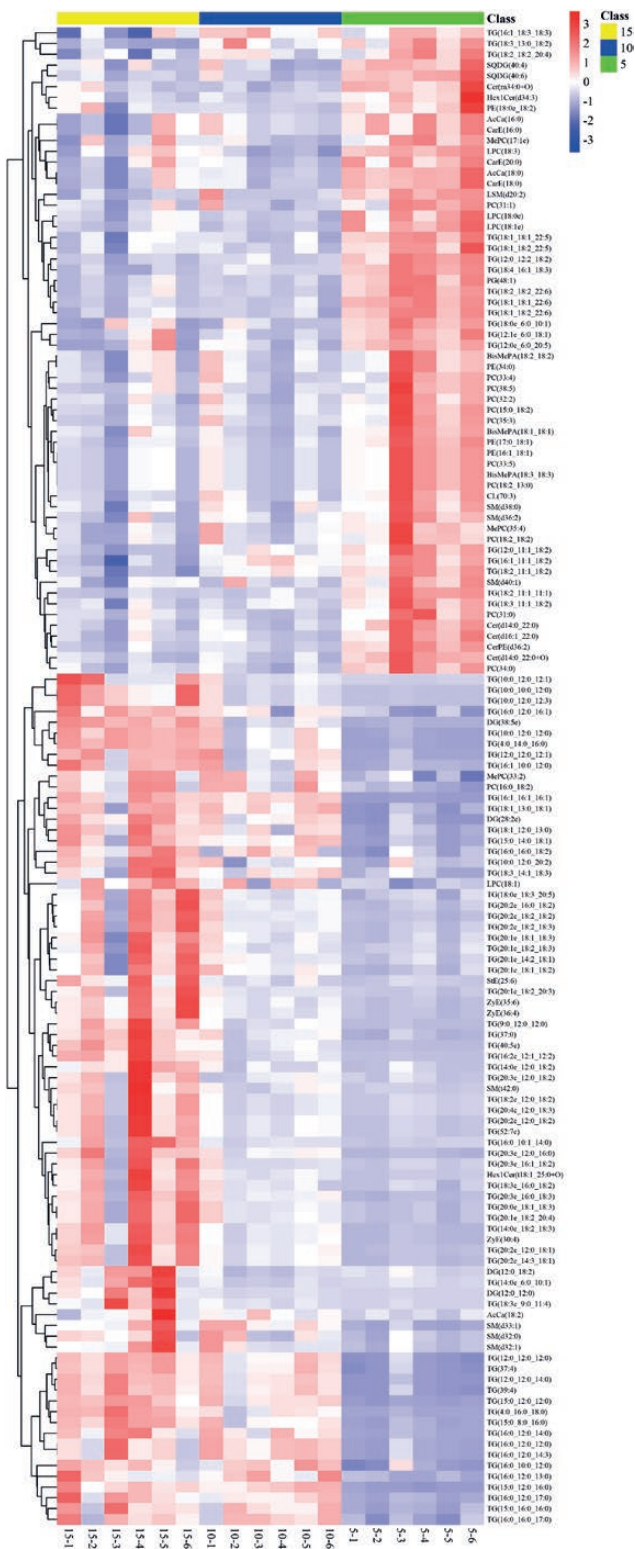
Fig. 4. Agglomerate hierarchical clustering results of potential lipid makers for discriminating *Hermetia illucens* larvae at different days of age.

explanation for this may be that FW contains a variety of animal and vegetable fat or oils. Another reasonable explanation for this may be that *H. illucens* belongs to insect, and its physiological function is limited, which the lipid profiles of the body reflect those of the diets (Ushakova et al. 2016, Ewald et al. 2020). Indeed, this was

supported by the fact that the lipid profiles of *H. illucens* were very similar to those of the diets in the present study (Table 1).

In the present study, the predominant lipid class in *H. illucens* larvae was TG, followed by PC and SM. This result was inconsistent with the reported in pork and chicken, in which the predominant lipid class was TG, PC, and PE (Mi et al. 2018, Mi et al. 2019). This may be closely related to the physiological function of the body and require further study. In addition, a large amount of GLs (TG and DG) were deposited during the growth and development of larvae. This result was consistent with the reported, which showed that the lipid deposition was mainly characterized by TG synthesis and concentration in lipid droplets (Hilgendorf et al. 2019). Most GPs (PC, PE, and PS) classes in 10- and 15-d-old larvae decreased, especially PC and PE in this study. The PC and PE are the major classes and proportion of GPs, serving as structural components, is relatively fixed (Wood et al. 2008). Similarly, the relative contents of GPs in pork decreased with the increase of age (Li et al. 2021a).

In the present study, the OPLS-DA model was robust, and overfitting did not occur because all Q^2 points were lower than the rightmost original Q^2 point, and the Q^2 intercept values were in the range of (0, −0.46) in ion mode (Li et al. 2021c). To differentiate the biomarkers of lipid molecules in larvae of different ages, the lipidomic data were analyzed by one-way ANOVA. A total of 139 significantly different lipids were identified, of which 79 upregulated and 60 downregulated in the 15-d-old vs. 10-d-old vs. 5-d-old groups. Notably, in 66 of the upregulated GL species, including 62 TGs and 4 DGs. This is consistent with the results in Table 1 showing that levels of TG and DG were significantly higher in the 15-d-old. Indeed, the developmental stages influenced the size distributions of the adipocytes (Park et al. 2018). In addition, larval stage would deposit a large amount of fat to accumulate energy for later development into adults (not eating) (Padmanabha et al. 2020). Interestingly, the significantly upregulated TGs were rich in saturated and monounsaturated fatty acids (SFAs and MUFAs) in the present study. The SFA and MUFA are mainly used for oxidation energy supply (Sargent et al. 2003). These findings indicated that *H. illucens* larvae accumulated a large amount of TG rich in SFAs and MUFAs during growth and development to accumulate energy for adult survival. In this study, 19 metabolic pathways were enriched based on 139 different lipid, among them 9 metabolic pathways closely related to lipids, main including GL and GP metabolisms. Previous study has shown that GL and GP metabolisms were the key metabolic pathways for the regulating of TG and phospholipids (Atsushi et al. 2014). Therefore, GL and GP metabolisms were considered to be the key pathway to regulate lipid deposition of *H. illucens* larvae during growth and development.

A systematic, in-depth lipidomics analysis was conducted on *H. illucens* larvae ranging in age from 5 to 15 d. Forty-three subclasses of 3,205 lipid molecules were identified in larvae, of which 139 significantly different lipids were identified during larvae growth. Interestingly, *H. illucens* larvae accumulated a large amount of TG rich in SFAs and MUFAs. The GL and GP metabolisms were considered to be the key pathway to regulate lipid deposition of *H. illucens* larvae. Consequently, LC-MS-based lipidomics provides a feasible strategy to analyze *H. illucens* larvae samples. To the best of our knowledge, this is the first work exploring the molecular-level mechanism of lipid deposition during the growth stage of *H. illucens* larvae. The findings provide novel insights into the nutritional value and comprehensive utilization of insect larvae.
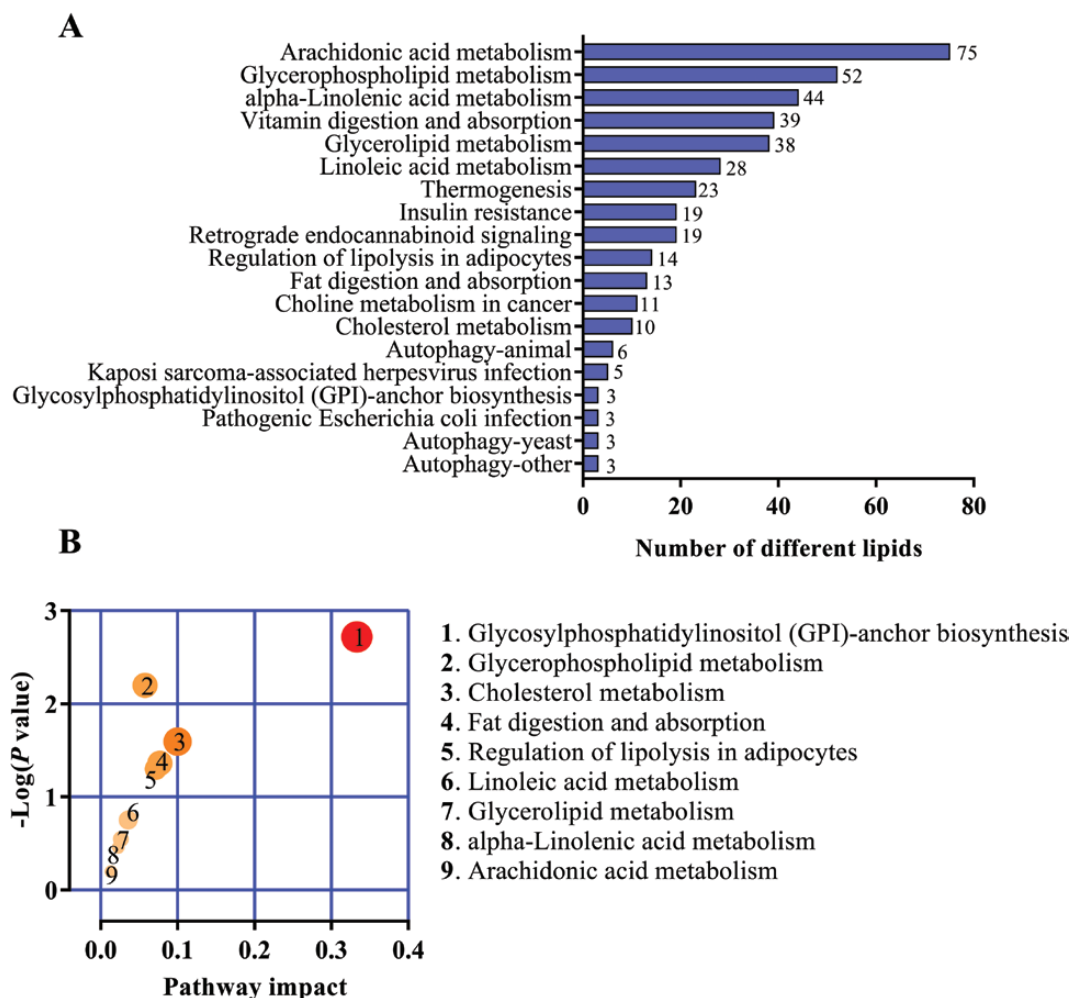
Fig. 5. Metabolic pathways involved in different lipids of larvae at different ages. (A) Enrichment pathways of different lipids. (B) Map of significant metabolic pathways related to lipids.

Supplementary Data

Supplementary data are available at *Journal of Insect Science* online.

Acknowledgments

Author Contributions

MML: Methodology, Writing-original draft, Resources, Data curation, Visualization. **GYW**: Methodology, Resources, Data curation, Visualization. **RSS**: Methodology, Data Curation, Writing (original draft). **QLX**, **JCZ** and **RS**: Validation, Data Curation. **LSL**: Supervision, Formal analysis, Writing-review & editing, Project administration.

References Cited

Atsushi, Y., H. Yasuhiro, M. Naoki, N.S. Yoko, O. Saori, T. Takashi, and S. Takayuki. 2014. Glycerophosphate/Acylglycerophosphate acyltransferases. Biology. 3: 801–830.

Belghit, I., N.S. Liland, P. Gjesdal, I. Biancarosa, E. Menchetti, Y. Li, R. Waagbø, Å. Krogdahl, and E. Lock, 2019. Black soldier fly larvae meal can replace fish meal in diets of sea-water phase Atlantic salmon (*Salmo salar*). Aquaculture. 503: 609–619.

Bosch, G., S. Zhang, D. Oonincx, and W. Hendriks, 2014. Protein quality of insects as potential ingredients for dog and cat foods. J. Nutr. Sci. 3: e29.

Chu, X., M. Li, G. Wang, K. Wang, R. Shang, Z. Wang, and L. Li, 2020. Evaluation of the low inclusion of full-fatted *Hermetia illucens* larvae meal for layer chickens: Growth performance, nutrient digestibility, and gut health. Front. Vet. Sci. 7: 962.

Dobermann, D., J. Swift, and L. Field, 2017. Opportunities and hurdles of edible insects for food and feed. Nutr. Bull. 42: 293–308.

El-Dakar, M.A., R.R. Ramzy, H. Ji, and M. Plath, 2020. Bioaccumulation of residual omega-3 fatty acids from industrial *Schizochytrium* microalgal waste using black soldier fly (*Hermetia illucens*) larvae. J. Clean. Prod. 268: 122288.

El-Dakar, M.A., R.R. Ramzy, M. Plath, and H. Ji, 2021. Evaluating the impact of bird manure vs. mammal manure on *Hermetia illucens* larvae. J. Clean. Prod. 278: 123570.

Ewald, N., A. Vidakovic, M. Langeland, A. Kiessling, S. Sampels, and C. Lalander, 2020. Fatty acid composition of black soldier fly larvae (*Hermetia illucens*)—possibilities and limitations for modification through diet. Waste Manage.. 102: 40–47.

Gerber, P.J., H. Steinfeld, B. Henderson, A. Mottet, C. Opio, J. Dijkman, A. Falcucci, and G. Tempio. 2013. Tackling climate change through livestock a global assessment of emissions and mitigation opportunities. FAO.

Griffiths, W.J. and Y. Wang. 2009. Analysis of neurosterols by GC-MS and LC-MS/MS. J. Chromatogr. B. 877: 2778–2805.

Guo, H., C. Jiang, Z. Zhang, W. Lu, and H. Wang. 2020. Material flow analysis and life cycle assessment of food waste bioconversion by black soldier fly larvae (*Hermetia illucens* L.). Sci. Total Environ. 750: 141656.

Gustavsson, J., C. Cederberg, and U. Sonesson. 2011. Global food losses and food waste. Save Food at Interpack Düsseldorf, Germany.

Haas, E., C. Wagner, A. Koelmans, M. Kraak, and W. Admiraal. 2006. Habitat selection by chironomid larvae: fast growth requires fast food. J. Anim. Ecol. 75: 148–155.

Han, X., 2016. Lipidomics for studying metabolism. Nat. Rev. Endocrinol. 12: 668–679.

Han, X. and R. Gross. 2003. Global analyses of cellular lipidomes directly from crude extracts of biological samples by ESI mass spectrometry: a bridge to lipidomics. J. Lipid Res. 44: 1071–1079.

He, M., Y. Sun, D. Zou, H. Yuan, B. Zhu, X. Li, and Y. Pang, 2012. Influence of temperature on hydrolysis acidification of food waste. Procedia Environ. Sci. 16: 85–94.

Hilgendorf, K.I., C.T. Johnson, A. Mezger, S.L. Rice, A.M. Norris, J. Demeter, W.J. Greenleaf, J.F. Reiter, D. Kopinke, and P.K. Jackson, 2019. Omega-3 fatty acids activate ciliary FFAR4 to control adipogenesis. Cell. 179: 1–17.

Lalander, C., S. Diener, C. Zurbrügg, and B. Vinnerås, 2019. Effects of feedstock on larval development and process efficiency in waste treatment with black soldier fly (*Hermetia illucens*). J. Clean. Prod. 286: 211–219.

Li, J., Y. Yang, T. Zhan, Q. Zhao, J. Zhang, X. Ao, J. He, J. Zhou, and C. Tang, 2021a. Effect of slaughter weight on carcass characteristics, meat quality, and lipidomics profiling in longissimus thoracis of finishing pigs. LWT. 140: 110705.

Li, M., M. Zhu, W. Chai, Y. Wang, D. Fan, M. Lv, X. Jiang, Y. Liu, Q. Wei, and C. Wang, 2021b. Determination of lipid profiles of Dezhou donkey meat using an LC-MS-based lipidomics method. J. Food Sci. 86: 4511–4521.

Li, M., M. Zhu, W. Chai, Y. Wang, Y. Song, B. Liu, C. Cai, Y. Song, X. Sun, P. Xue, and C. Wang, 2021c. Determination of the heterogeneity of intramuscular fat and visceral adipose tissue from Dezhou donkey by lipidomics and transcriptomics profiling. Front. Nutr. 8:746684.

Mi, S., K. Shang, W. Jia, C. Zhang, X. Li, Y. Fan, and H. Wang, 2018. Characterization and discrimination of Taihe black-boned silky fowl (*Gallus gallus domesticus* Brisson) muscles using LC/MS-based lipidomics. Food Res. Int. 109: 187–195.

Mi, S., K. Shang, X. Li, C. Zhang, J. Liu, and D. Huang, 2019. Characterization and discrimination of selected China's domestic pork using an LC-MS-based lipidomics approach. Food Control. 100: 305–314.

Padmanabha, M., A. Kobelski, A. Hempel, and S. Streif, 2020. A comprehensive dynamic growth and development model of *Hermetia illucens* larvae. PLoS One. 15: e239084.

Parfitt, J., M. Barthel, and S. Macnaughton, 2010. Food waste within food supply chains: quantification and potential for change to 2050.

Philosophical transactions of the Royal Society of London. Series B, Biological sciences. 365: 3065–3081.

Park, S.J., S. Beak, D.J.S. Jung, S.Y. Kim, I.H. Jeong, M.Y. Piao, H.J. Kang, D.M. Fassah, S.W. Na, S.P. Yoo, and M. Baik, 2018. Genetic, management, and nutritional factors affecting intramuscular fat deposition in beef cattle-a review. Asian-Australas. J. Anim. Sci.. 31: 1043–1061.

Philippe, F.X. and B. Nicks, 2015. Review on greenhouse gas emissions from pig houses: production of carbon dioxide, methane and nitrous oxide by animals and manure. Agr. Ecosyst. Environ. 199: 10–25.

Rabani, V., H. Cheatsazan, and S. Davani, 2019. Proteomics and lipidomics of black soldier fly (Diptera: Stratiomyidae) and blow fly (Diptera: Calliphoridae) larvae. J. Insect Sci. 19: 1–9.

Salomone, R., G. Saija, G. Mondello, A. Giannetto, S. Fasulo, and D. Savastano, 2017. Environmental impact of food waste bioconversion by insects: application of life cycle assessment to process using *Hermetia illucens*. J. Clean. Prod. 140: 890–905.

Sargent, J.R., D.R. Tocher, and J.G. Bell, 2003. The lipids. Fish Nutrition. 3: 181–257.

Sun, T., X. Wang, P. Cong, J. Xu, and C. Xue, 2020. Mass spectrometry-based lipidomics in food science and nutritional health: a comprehensive review. Compr. Rev. Food Sci. F. 19: 2530–2558.

Surendra, K.C., J.K. Tomberlin, A. van Huis, J.A. Cammack, L.L. Heckmann, and S.K. Khanal, 2020. Rethinking organic wastes bioconversion: evaluating the potential of the black soldier fly (*Hermetia illucens* (L.)) (Diptera: Stratiomyidae) (BSF). Waste Manage.. 117: 58–80.

Trinh, T.X.N., K.T. Jeffery, and V. Sherah, 2013. Influence of resources on *Hermetia illucens*. (Diptera: Stratiomyidae) larval development. J. Med. Entomol. 50: 898–906.

Uçkun Kiran, E., A.P. Trzcinski, W.J. Ng, and Y. Liu, 2014. Bioconversion of food waste to energy: a review. Fuel. 134: 389–399.

Ushakova, N.A., E.S. Brodskii, A.A. Kovalenko, A.I. Bastrakov, A.A. Kozlova, and D.S. Pavlov, 2016. Characteristics of lipid fractions of larvae of the black soldier fly *Hermetia illucens*. Dokl. Biochem. Biophys. 468: 209–212.

Wang, Y. and M. Shelomi, 2017. Review of black soldier fly (*Hermetia illucens*) as animal feed and human food. Foods. 6: 91.

Wang, S.Y., L. Wu, B. Li, and D. Zhang, 2019. Reproductive potential and nutritional composition of *Hermetia illucens* (Diptera: Stratiomyidae) prepupae reared on different organic wastes. J. Econ. Entomol. 113: 527–537.

Wood, J.D., M. Enser, A.V. Fisher, G.R. Nute, P.R. Sheard, R.I. Richardson, S.I. Hughes, and F.M. Whittington, 2008. Fat deposition, fatty acid composition and meat quality: a review. Meat Sci.. 78: 343–358.

Xu, F., Y. Li, X. Ge, L. Yang, and Y. Li, 2018. Anaerobic digestion of food waste – challenges and opportunities. Bioresource Technol. 247: 1047–1058.

Yu, M., Z. Li, W. Chen, T. Rong, G. Wang, J. Li, and X. Ma, 2019. Use of *Hermetia illucens* larvae as a dietary protein source: effects on growth performance, carcass traits, and meat quality in finishing pigs. Meat Sci. 158: 107837.